I dont know yet

Faustmann Christian

Faculty of Physics
Technical University of Vienna

This thesis is submitted for the degree of
Bachelor of Science

TU Vienna September 2017

Introduction

One of Prof. Rauschenbeutel projects uses a novel type of whispering-gallery-mode (WGM) resonator interfaced via nanowaveguides and coupled to single Rubidium atoms to carry out experiments in the realm of Cavity Quantum Electrodynamics. The WGM resonator is a so-called bottle-microresonator (BMR) manufactured from a standard optical glass fiber in a heat and pull process. The light is radially confined inside the resonator by total internal reflection and propagates along the circumference of the resonator. In such a structure, a signicant fraction of the light field propagates in the evanescent field. By overlapping this field with the evanescent field of an optical nanofiber, light can be coupled into and out of the resonator very efficiently. Due to the extremely low absorption of silica (and low surface roughness) we can produce bottle-resonators with ultra-high optical Q-factor exceeding 10^8. Rubidium atoms are delivered to the resonator using an atomic fountain. When the atoms enter the vicinity of the WGM, and they are in the evanescent field they can be coupled to the light. For the moment the atoms are only flying by the resonator, but only for ~2 µs and moreover the distance between the resonator and the atom is not controlled. This prevents the realization from more complicated experiments. For that reason one needs to trap the atom. The choice made to trap the atom is to use a dipole trap (see chapter 1), which is a conservative trap. Because the atoms have a velocity dispersion, we do not know in advance when and where the atoms enter the evanescent field. For that we need to consider that they arrive with some kinetic energy $\Rightarrow$ trap depth $\gg E_{kin}$.
The aim of this Bachelor thesis is to elaborate all the parameters needed to realise the trap.

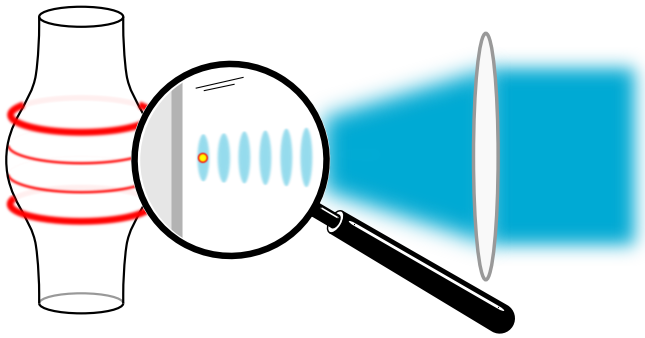

Table of contents

List of figures **vii**

List of tables **ix**

1 Theory of laser trapping of atoms **1**

2 Absorption of photon by an atom **7**
2.1 Laser interactions - Two-level atom 7
2.2 Basic laser absorption spectroscopy 9
2.3 Laser absorption 9
2.4 Doppler shifts 10
2.5 Absorption coefficient - weak field 11
2.6 Population 12
2.7 Absorption coefficient - general case 14
2.8 Non-linear differential equation 15
2.9 Data table 16
2.10 D2 line 17

3 Experiment **19**
3.1 Setup & Tools 19
3.2 Laser diameter measurement 19
3.3 Power / intensity measurement 19
3.4 Doppler-free measurement 19

4 Evaluation **21**
4.1 Data processing 21
4.2 Temperature & saturation intensity 21
4.3 Comparison with theory 21
4.4 Compare Doppler-free measurement with theoretical values 21

References **23**

Appendix A Theory **25**

Appendix B Experiment **27**

Appendix C Evaluation **29**

List of figures

1.1 Illustration of dipole traps with red and blue detuning. 1
1.2 1D Intensity distribution of a retroreflected gaussian laser beam. 2
1.3 Experimental setup and intensity distribution. 3
1.4 Overlap of Dipole and Van-der-Waals potential. 4
1.5 Trap depth for different detuning. 4
1.6 Calculated trap potential for 20 mW power and a 6 GHz detuning. 4

2.1 Two-level atom model 7
2.2 The Lorentzian line shape profile for resonance absorption 8
2.3 Basic arrangement for ordinary laser absorption spectroscopy. 9
2.4 The Lorentzian compared to the Gaussian profile 12
2.5 $5^2S_{1/2} \rightarrow 6^2P_{3/2}$ transition of ^{85}Rb and ^{87}Rb with corresponding hyperfine structure 17
2.6 Doppler spectrum of D2 line 17
2.7 Relative energy gaps of the groundstates between both isotopes 18

List of tables

2.1 Properties of rubidium isotopes 16

Chapter 1

Theory of laser trapping of atoms

Atoms can be trapped in a optical potential created by the dispersive interaction of the atomic dipole moment with the intensity gradient of the light field. These trap can be used to confine the atoms in 3D, and to counter gravity. In the case of large detunings the expression for the dipole potential and scattering rate [1] is the following:

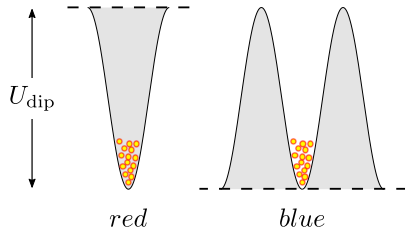

Fig. 1.1 Illustration of dipole traps with red and blue detuning.

$$U_{\text{dip}}(z) = \frac{3\pi c^2}{2\omega_0^3}\,\frac{\Gamma}{\Delta}\,I(z)\ , \tag{1.1}$$

$$\Gamma_{\text{sc}}(z) = \frac{3\pi c^2}{2\hbar\omega_0^3}\left(\frac{\Gamma}{\Delta}\right)^2 I(z)\ . \tag{1.2}$$

Where c is the speed of light, Γ is the transition rate for an atom in the excited state to decay to the ground state, $\omega_0 = 2\pi\ \frac{c}{\lambda} = 2\pi\nu$, Δ is the detuning between the light and the atomic transition ($\Delta := \omega - \omega_0$), where ω is the driving frequency of the light field and $I(z)$ corresponds to the intensity at a given distance to the resonator. Dipole traps can be divided into two main classes, red-detuned traps ("red" detuning, $\Delta < 0$) and blue-detuned traps ("blue" detuning, $\Delta > 0$). Below an atomic resonance the dipole potential is negative and the potential minima are therefore found at positions with maximum intensity and potential minima correspond to minima of the intensity and the ??? repels atoms from the field??? as seen in Fig. 1.1.

For our case there are three different red-detuned trap configurations possible: *Focused-beam traps* consisting of a single beam, the *crossed-beam traps* created by two or more beams intersecting at their foci, and *standing-wave traps* where atoms are axially confined in the antinodes of a standing wave. For our Experiment it is important that the atoms are as close as possible from the resonator, because the interacting evanescent field of the photon in the

resonator decreases exponentially with a decay length of $\frac{\lambda_{at}}{2\pi}$ where λ_{at} is the wavelength of the atomic transition. 780 nm for the D_2 line $5S_{1/2} \rightarrow 5P_{3/2}$ of Rb.

The closest trap potential provides a retroreflected gaussian beam with a distance of $\frac{\lambda_{laser}}{4}$ at the first minimum of the standing wave (see Fig. 1.2). If one uses a laser closely detuned from the D_2 line $5S_{1/2} \rightarrow 5P_{3/2}$, i.e. @ 783 nm, which leads to a distance of $\frac{\lambda}{4} \approx 190$ nm, but this would be to far from the resonator. For rubidium it is possible to use alternatively a laser close to the $5S_{1/2} \rightarrow 6P_{3/2}$ @ 420 nm, this would reduce the distance to the resonator to 105 nm.

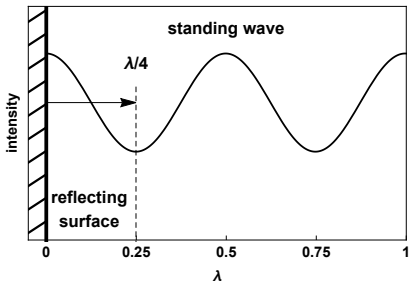

Fig. 1.2 1D Intensity distribution of a retroreflected gaussian laser beam.

As we can see in (1.1) the dipole potential is $\sim \frac{I}{\Delta}$. To condition our setup properly we have to consider some constraints. Laser power is limited and additionally we do not want to send too much power onto the resonator, because of safety precautions. On the other hand we want to keep the scattering rate as low as possible, which is $\sim \frac{I}{\Delta^2}$. However if $\Delta <$ separation between D_1 & D_2 lines (420 & 421 nm) then we need to take the fine structure into account and for that equation (1.1) isn't sufficient enough. In our case we are red-detuned from the D_2-transition and the detuning will be smaller than the fine structure splitting of 2.32 THz, so we get an additional counter term of the D_1-transition (blue-detuned):

$$U_{\mathrm{dip}}(z) = \frac{\pi c^2}{2\omega_0^3} \left(\frac{2\,\Gamma_{\omega,D2}}{\Delta_{D2}} + \frac{\Gamma_{\omega,D1}}{\Delta_{D1}} \right) I(z) \,, \tag{1.3}$$

$$\Gamma_{\mathrm{sc}}(z) = \frac{\pi c^2}{2\hbar\omega_0^3} \left(\frac{2\,\Gamma_{\omega,D2}\,\Gamma_{\omega,D2,tot}}{\Delta_{D2}^2} + \frac{\Gamma_{\omega,D1}\,\Gamma_{\omega,D1,tot}}{\Delta_{D1}^2} \right) I(z) \,. \tag{1.4}$$

$\Gamma_{\omega,Dx}$ are the transition rates from $6P_{1/2}$ for the D_1 line and accordantly $6P_{3/2}$ for the D_2 line to decay to $5S_{1/2}$, $\Gamma_{\omega,Dx,tot}$ are the transition rates from $6P_{1/2}$&$6P_{3/2}$ over all their decay channels with $\frac{1}{\Gamma_{\omega,Dx,tot}}$ is the mean lifetime of the state and Δ_{Dx} represents $\omega - \omega_{0,Dx}$. All values can be found in table 2.1.

Possible configuration of optical dipole trap

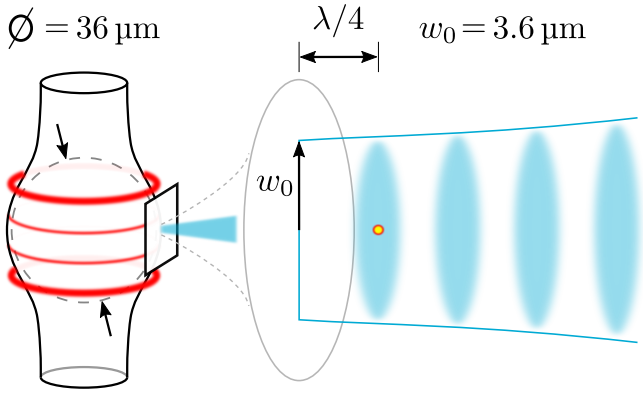

Fig. 1.3 Experimental setup and intensity distribution.

Our goal is to trap the free falling atoms as close as possible to the resonator by simultaneously low scattering rate and without damaging the resonator with the incoming laser beam. To calculate the trap potential we have to derive the intensity for a gaussian beam, but to get the intensity one has to calculate the electric field first. One considers that the beam is enough focused on the resonator that the reflecting surface is more or less "flat" (see Fig. 1.3). With this assumption the electric field becomes:

$$\hat{E}(z) = \hat{x}\ \left(e^{-ik_z z} + re^{ik_z z}\right) \tag{1.5}$$

with r as the reflection coefficient, which is in case of our resonator surface $r = -0.02$. This leads to the intensity:

$$I(z) = \frac{\left|\hat{E}(z)\right|^2}{2\eta} = I_0\left[1 + r^2 + 2r\cos\left(\frac{2\omega}{c}\ z\right)\right]\ . \tag{1.6}$$

Where $I_0 = \frac{{E_0}^2}{2\eta}$ and ω is the driving frequency of the laser. For further calculation we need the dipole potential dependent from the laser power. The power of a gaussian beam is defined as:

$$P_0 = \frac{1}{2}\ I_0 {w_0}^2 \pi \tag{1.7}$$

with w_0 as the beam radius, which is for our setup $w_0 = 3.6\,\mu\text{m}$ as pictured in Fig. 1.3. To have only one parameter to adjust we will choose a power between $0 < P < 80\,\text{mW}$. The trap depth must be bigger than the energy of the atom, here the kinetic energy $E_{kin} = \frac{1}{2} m_{Rb} v^2$ due to the fact that the atoms are free falling for between 0 and 60 ms would be in terms of temperature $E_{kin}/k_B = 1.77\,\text{mK}$. Our trap without cooling is conservative, this means the captured atoms keep there energy. If now an atom is not captured in the middle of the

potential well it gains additional potential energy and it's total energy increases. It is then possible that the atom can escape the trap. Therefore one should add a safety margin to capture more atoms. For example a 5 mK trap would capture $\frac{5-1.77}{5}$ 100 % ≈ 60 % of atoms entering the trap in the worst case, because atoms have $E_{kin}/k_B < 1.77\,\text{mK}$. In our setup we are so close to the resonator that we have to consider a Van-der-Waals potential, which reduces our first potential barrier (see Fig. 1.4).

To determine a correct detuning for our trap we will use the combination of both potentials in all further calculations. The depth of the potential well is now the difference between the reduced first maximum and the first minimum at $\lambda/4$. As we can see in Fig. 1.5 the detuning has to be lower than 7 GHz. For a detuning of 6 GHz we get a trap depth of 5.5 mK as shown in Fig. 1.6 .

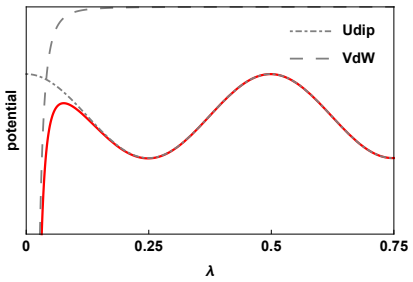

Fig. 1.4 Overlap of Dipole and Van-der-Waals potential.

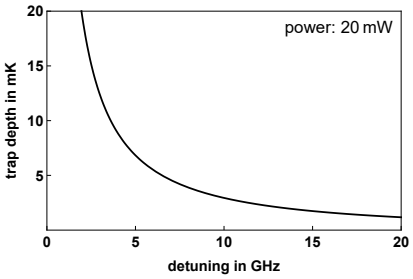

Fig. 1.5 Trap depth for different detuning.

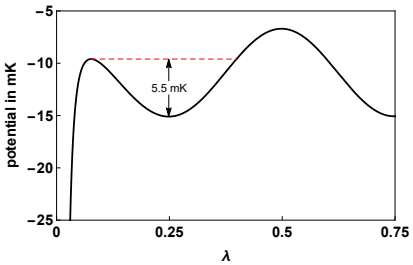

Fig. 1.6 Calculated trap potential for 20 mW power and a 6 GHz detuning.

This requires to see the transitions to have a reference to lock the laser afterwards. To determine

$\Gamma_{\omega,420nm-Line}$ we can use a theoretical relation with the intensity saturation, which has to be checked by our measurement:

$$I_{s,420} = \frac{\Gamma_{\omega,tot,420} \cdot {\omega_{420}}^3 \cdot I_{s,780}}{\Gamma_{\omega,420} \cdot \Gamma_{\omega,780} \cdot {\omega_{780}}^3} \tag{1.8}$$

$$\text{with} \quad \Gamma_{\omega,tot,420} = \frac{1}{total\ lifetime\ of\ 6P_{3/2}\ state}$$

$\Rightarrow$ We want to measure I_s for the blue 420.29 nm-line.

Chapter 2

Absorption of photon by an atom

The purpose of this section is to outline the basic features observed in saturated absorption spectroscopy and relate them to simple atomic and laser physics principles. For this we will follow the guidance of [2] and [3].

A Atomic spectrum is composed of several absorption lines, but usually well separated. So if we are close to one line absorption of light by another line is negligible. In that case the system can be described by a two-level atom, which we will use in the further sections.

2.1 Laser interactions - Two-level atom

We begin with the interaction between a laser field and a sample of stationary atoms having only two possible energy levels. Aspects of thermal motion will be treated subsequently. The difference $\Delta E = E_1 - E_0$ between the excited state $|e\rangle$ energy E_1 and ground state $|g\rangle$ energy E_0 is used with Planck's law to determine the photon frequency ν associated with transitions between the two states:

$$\Delta E = h\nu_0 \tag{2.1}$$

There are three transition processes involving atoms and laser fields:

(1) absorption

(2) spontaneous emission

(3) stimulated emission

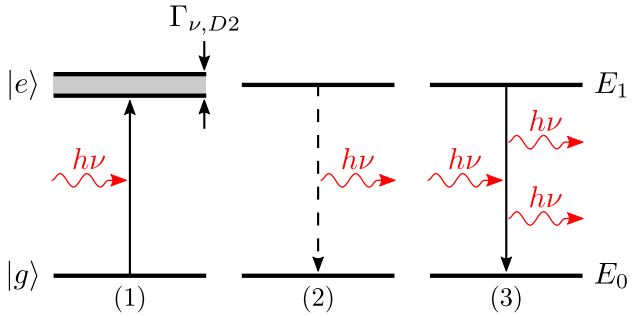

Fig. 2.1 Two-level atom model

We consider spontaneous emission first – a process characterized by a transition rate or probability per unit time for an atom in the excited state to decay to the ground state. This transition rate will be denoted Γ_ω and is about $2\pi \cdot 1.3\,\mathrm{MHz}$ for the rubidium levels studied here.

In the absence of an external field, any initial population of excited state atoms would decay exponentially to the ground state with a mean life time $\Delta t = 1/\Gamma_\omega \approx 122\,\mathrm{ns}$. In the rest frame of the atom, spontaneous photons are emitted in all directions with an energy spectrum having a mean $E = h\nu_0$ and a full width at half maximum (FWHM) ΔE given by the Heisenberg uncertainty principle $\Delta E \Delta t = \hbar$ or $\Delta E = \Gamma_\omega \hbar$. Expressed in frequency units, the FWHM is called the *natural linewidth* and given the symbol Γ_ν. Thus

$$\Gamma_\nu = \frac{\Gamma_\omega}{2\pi} \tag{2.2}$$

For our rubidium levels, $\Delta E \approx 5.4 \cdot 10^{-9}\,\mathrm{eV}$ or $\Gamma_\nu \approx 1.3\,\mathrm{MHz}$.

The stimulated emission and absorption processes are also described by a transition rate – a single rate giving the probability per unit time for a ground state atom to absorb a laser photon or for an excited state atom to emit a laser photon. The stimulated transition rate is proportional to the laser intensity I (SI units of $\mathrm{W\,m^{-2}}$) and is only significantly different from zero when the laser frequency ν is near the resonance frequency ν_0. This transition rate will be denoted αI, where

$$\alpha = \alpha_0 \mathcal{L}(\nu, \nu_0) \tag{2.3}$$

and

$$\mathcal{L}(\nu, \nu_0) = \frac{1}{1 + 4(\nu - \nu_0)^2 / {\Gamma_\nu}^2} \tag{2.4}$$

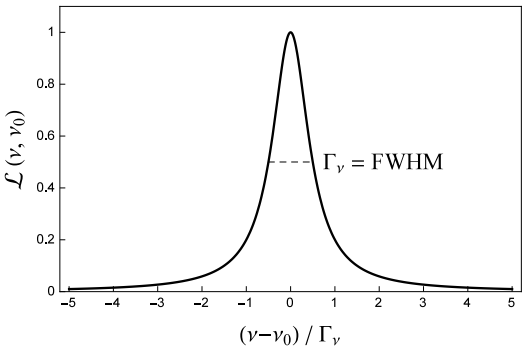

Fig. 2.2 The Lorentzian line shape profile for resonance absorption

gives the *Lorentzian* frequency dependence as shown in Fig. 2.2. $\mathcal{L}(\nu, \nu_0)$ also describes the spectrum of radiation from spontaneous emission and the width Γ_ν is the same for both cases. The maximum transition rate $\alpha_0 I$ occurs right on resonance ($\nu = \nu_0$).

The value of Γ_ω / α_0 defines the saturation intensity I_s of the atoms. Its significance is that when the laser intensity is equal to the saturation intensity, excited state atoms are equally likely to decay by stimulated emission or by spontaneous emission.

2.2 Basic laser absorption spectroscopy

The basic arrangement for ordinary laser absorption spectroscopy through a gaseous sample is shown in Fig. 2.3. A laser beam passes through the vapor cell and its intensity is measured by a photodiode detector as the laser frequency ν is scanned through the natural resonance frequency.

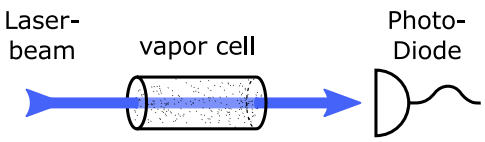

Fig. 2.3 Basic arrangement for ordinary laser absorption spectroscopy.

When a laser beam propagates through a gaseous sample, the two stimulated transition processes change the intensity of the laser beam and affect the density of atoms in the ground and excited states. To get a better understanding of absorption spectroscopy we begin with the basic equation describing how the laser intensity changes as it propagates through the sample and then continue with the effects of Doppler shifts and population changes.

2.3 Laser absorption

Because of stimulated emission and absorption, the laser intensity $I(x)$ varies as it propagates from x to $x + \mathrm{d}x$ in the medium. The following equation describes this process:

$$I(x + \mathrm{d}x) - I(x) = -I(x) h\nu\alpha n_0 (P_0 - P_1)\mathrm{d}x \tag{2.5}$$

where:

n_0 ... atom density

$n_0 P_0$ ... proportion of atoms in $|g\rangle$

$n_0 P_1$ ... proportion of atoms in $|e\rangle$

Equation 2.5 leads to

$$\frac{\mathrm{d}I}{\mathrm{d}x} = -\kappa I \tag{2.6}$$

where the *absorption coefficient* (fractional absorption per unit length)

$$\kappa = h\nu n_0 \alpha (P_0 - P_1) \tag{2.7}$$

The proportionality to $P_0 - P_1$ arises from the competition between stimulated emission and absorption and it is important to appreciate the consequences. If there are equal numbers of atoms in the ground and excited state ($P_0 - P_1 = 0$), laser photons are as likely to be

emitted by an atom in the excited state as they are to be absorbed by an atom in the ground state and there will be no attenuation of the incident beam. The attenuation maximizes when all atoms are in the ground state ($P_0 - P_1 = 1$) because only upward transitions would be possible. And the attenuation can even reverse sign (become an amplification as it does in laser gain media) if there are more atoms in the excited state ($P_0 > P_1$).

2.4 Doppler shifts

Atoms in a vapor cell move randomly in all directions with each component of velocity having a distribution of values. Only the component of velocity parallel to the laser beam direction will be important when taking into account Doppler shifts and it is this component we refer to with the symbol v. The density of atoms $\mathrm{d}n$ in the velocity group between v and $v + \mathrm{d}v$ is given by the Boltzmann velocity distribution:

$$\mathrm{d}n = n_0 \sqrt{\frac{m}{2\pi k_B T}} \exp\left(-\frac{mv^2}{2k_B T}\right) \mathrm{d}v \tag{2.8}$$

With a standard deviation given by:

$$\sigma_v = \sqrt{\frac{k_B T}{m}} \tag{2.9}$$

This is just a standard Gaussian distribution

$$\mathrm{d}n = n_0 \frac{1}{\sqrt{2\pi}\sigma_v} \exp\left(-\frac{v^2}{2{\sigma_v}^2}\right) \mathrm{d}v \tag{2.10}$$

with a mean of zero – indicating the atoms are equally likely to be going in either direction. It is properly normalized so that the integral over all velocities ($-\infty \to \infty$) is n_0, the overall atom density.

Atoms moving with a velocity v see the laser beam Doppler shifted by the amount $\nu(v/c)$. We will take an equivalent, alternate view that atoms moving with a velocity v have a Doppler shifted resonance frequency

$$\nu_0' = \nu_0 \left(1 + \frac{v}{c}\right) \tag{2.11}$$

in the lab frame. The sign has been chosen to be correct for a laser beam propagating in the positive direction so that the resonance frequency is blue shifted to higher frequencies if v is positive and red shifted if v is negative.

The absorption coefficient $\mathrm{d}\kappa$ from a velocity group $\mathrm{d}n$ at a laser frequency ν is then obtained from Eq. 2.7 by substituting $\mathrm{d}n$ for n_0 and by adjusting the Lorentzian dependence of α so

that it is centered on the Doppler shifted resonance frequency ν_0' (Eq. 2.11).

$$\mathrm{d}\kappa = h\nu\alpha_0(P_0 - P_1)\mathcal{L}(\nu, \nu_0')\mathrm{d}n \tag{2.12}$$

The absorption coefficient from all atoms is then found by integrating over all velocity groups.

2.5 Absorption coefficient - weak field

We treat the weak-laser case first where we have a very low intensity compared to I_s and therefore nearly all atoms will be in the ground state, i.e., $P_0 - P_1 = 1$ so that

$$\mathrm{d}\kappa = h\nu\alpha_0 n_0 \frac{1}{\sqrt{2\pi}\sigma_v}\mathcal{L}(\nu, \nu_0')\exp\left(-\frac{v^2}{2{\sigma_v}^2}\right)\mathrm{d}v \tag{2.13}$$

and

$$\kappa = \underbrace{h\nu\alpha_0 n_0 \frac{1}{\sqrt{2\pi}\sigma_v}}_{\beta}\int_{-\infty}^{\infty} \frac{1}{1 + 4\left[\nu - \nu_0\left(1 + \frac{v}{c}\right)\right]^2/{\Gamma_\nu}^2}\exp\left(-\frac{v^2}{2{\sigma_v}^2}\right)\mathrm{d}v \tag{2.14}$$

After the variable transformation

$$\left|\begin{array}{l} \nu_0' = \nu_0\left(1 + \dfrac{v}{c}\right) \\ v = \left(\dfrac{\nu_0'}{\nu_0} - 1\right)c = \left(\dfrac{\nu_0' - \nu_0}{\nu_0}c\right) \\ \mathrm{d}v = \dfrac{c}{\nu_0}\,\mathrm{d}\nu_0' \end{array}\right| = \beta\,\frac{c}{\nu_0}\int_{-\infty}^{\infty} \frac{1}{1 + 4(\nu - \nu_0')^2/{\Gamma_\nu}^2}\exp\left(-\frac{(\nu_0' - \nu_0)^2c^2}{2{\nu_0}^2{\sigma_v}^2}\right)\mathrm{d}\nu_0'$$

and substitution $\sigma_\nu = \frac{\nu_0}{c}\sigma_v$ we get

$$= \beta\,\frac{c}{\nu_0}\int_{-\infty}^{\infty} \frac{1}{1 + 4(\nu - \nu_0')^2/{\Gamma_\nu}^2}\exp\left(-\frac{(\nu_0' - \nu_0)^2}{2{\sigma_\nu}^2}\right)\mathrm{d}\nu_0' \tag{2.15}$$

Now we compare the width parameters from the Lorentzian (see table 2.1) with the Gaussian function for a temperature of 100 °C:

$$\sigma_\nu = \frac{c}{\lambda_{\mathrm{D2}}}\sqrt{\frac{k_B T}{m_{Rb85}c^2}} \approx 455\,\mathrm{MHz}$$

$$\Gamma_{\nu,\mathrm{D2}} = 0.282\,\mathrm{MHz}$$

$$\Rightarrow \Gamma_{\nu,\mathrm{D2}} \ll 2 \cdot \sigma_\nu$$

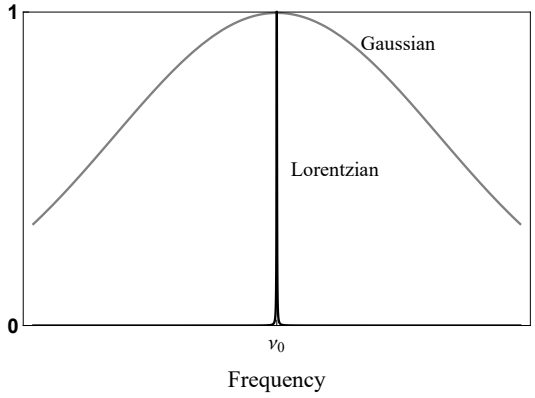

Fig. 2.4 The Lorentzian compared to the Gaussian profile

As we can see the Lorentzian function is significantly different from zero only within a very narrow range. Consequently the Gaussian remains relatively constant over the width of $\Gamma_{\nu,\mathrm{D2}}$. Therefore Eq. (2.15) can be accurately determined as the integral of the Lorentzian times the value of the exponential at $\nu_0' = \nu$:

$$= \beta\ \frac{c}{\nu_0}\exp\left(-\frac{(\nu-\nu_0)^2}{2{\sigma_\nu}^2}\right)\int_{-\infty}^{\infty}\frac{1}{1+4(\nu-\nu_0')^2/{\Gamma_\nu}^2}\mathrm{d}\nu_0' \tag{2.16}$$

and with the solution of the Lorentzian integral

$$\int_{-\infty}^{\infty}\mathcal{L}(\nu,\nu_0')\mathrm{d}\nu_0' = \frac{\pi\Gamma_\nu}{2} \tag{2.17}$$

we finally get the absorption coefficient in a weak field

$$\kappa = \kappa_0\exp\left(-\frac{(\nu-\nu_0)^2}{2{\sigma_\nu}^2}\right)\ \text{ with }\ \kappa_0 = h\nu\alpha_0 n_0\frac{1}{\sqrt{2\pi}\sigma_\nu}\frac{\pi\Gamma_\nu}{2} \tag{2.18}$$

2.6 Population

Before we can determine the general case of the absorption coefficient we need an expression for $P_0 - P_1$. For that we have to take into account the changes to the ground and excited state populations arising from a laser beam propagating through the cell. The rate equations for the ground and excited state probabilities or fractions become:

$$\begin{aligned}\frac{\mathrm{d}P_0}{\mathrm{d}t} &= \Gamma_\omega P_1 - \alpha I(P_0 - P_1)\\ \frac{\mathrm{d}P_1}{\mathrm{d}t} &= -\Gamma_\omega P_1 + \alpha I(P_0 - P_1)\end{aligned} \tag{2.19}$$

where the first term on the right in each equation arises from spontaneous emission and the second term arises from stimulated absorption and emission.
Considering $P_0 + P_1 = 1$ and the steady state condition

$$\frac{\mathrm{d}P_0}{\mathrm{d}t} = \frac{\mathrm{d}P_1}{\mathrm{d}t} = 0 \tag{2.20}$$

we get for the populations

$$P_0 = \frac{\Gamma_\omega + \alpha I}{\Gamma_\omega + 2\alpha I} \; ; \qquad P_1 = \frac{\alpha I}{\Gamma_\omega + 2\alpha I} \tag{2.21}$$

which leads to

$$(P_0 - P_1) = \frac{\Gamma_\omega}{\Gamma_\omega + 2\alpha I} \tag{2.22}$$

As we can see the population difference is dependent on Γ_ω (spontaneous decay rate), which is related to the *Lorentzian width parameter* Γ_ν. To combine the Lorentzians in α and $P_0 - P_1$ we rewrite both expressions with Eq. 2.2 and $\Delta\nu = 2(\nu - \nu_0)$:

$$\alpha = \alpha_0 \frac{1}{1 + \Delta\nu^2/{\Gamma_\nu}^2} = \alpha_0 \frac{\Gamma_\nu^2}{\Gamma_\nu^2 + \Delta\nu^2} \; ; \qquad (P_0 - P_1) = \frac{2\pi\Gamma_\nu}{2\pi\Gamma_\nu + 2\alpha I} \tag{2.23}$$

and get

$$(P_0 - P_1)\alpha = \frac{2\pi\Gamma_\nu}{2\pi\Gamma_\nu + 2I\alpha_0 \frac{\Gamma_\nu^2}{\Gamma_\nu^2 + \Delta\nu^2}} \; \alpha_0 \frac{\Gamma_\nu^2}{\Gamma_\nu^2 + \Delta\nu^2} = \frac{\alpha_0 \pi \Gamma_\nu^2}{\pi(\Gamma_\nu^2 + \Delta\nu^2) + I\alpha_0\Gamma_\nu} \tag{2.24}$$

dividing with $\pi\Gamma_\nu$ and substitute in the denominator α_0 with the definition of $I_s = 2\pi\Gamma_\nu/\alpha_0$ leads to

$$\alpha_0 \frac{1}{1 + \frac{\Delta\nu^2}{\Gamma_\nu} + \frac{2I}{I_s}} = \frac{\alpha_0}{(1 + \frac{2I}{I_s})} \; \frac{1}{1 + \frac{\Delta\nu^2}{\Gamma_\nu^2(1 + \frac{2I}{I_s})}} \tag{2.25}$$

with the definition of the power-broadened *width parameter*

$$\Gamma'_\nu = \Gamma_\nu \sqrt{1 + 2I/I_s} \tag{2.26}$$

we obtain

$$(P_0 - P_1)\alpha = \frac{\alpha_0}{(1 + \frac{2I}{I_s})} \; \mathcal{L}'(\nu, \nu_0) \quad \text{and} \quad \mathcal{L}'(\nu, \nu_0) = \frac{1}{1 + \frac{4(\nu - \nu_0)^2}{{\Gamma'_\nu}^2}} \tag{2.27}$$

2.7 Absorption coefficient - general case

For the general case we take now into account the velocity groups and their corresponding Doppler shifts for the case $P_0 - P_1 \neq 1$ and therefore

$$\mathrm{d}\kappa = h\nu n_0 \frac{\alpha_0}{(1+\frac{2I}{I_s})} \frac{1}{\sqrt{2\pi}\sigma_v} \mathcal{L}'(\nu, \nu_0') \exp\left(-\frac{v^2}{2{\sigma_v}^2}\right) \mathrm{d}v \tag{2.28}$$

and

$$\kappa = h\nu n_0 \frac{\alpha_0}{(1+\frac{2I}{I_s})} \frac{1}{\sqrt{2\pi}\sigma_v} \int_{-\infty}^{\infty} \frac{1}{1+4\left[\nu-\nu_0\left(1+\frac{v}{c}\right)\right]^2/{\Gamma_\nu'}^2} \exp\left(-\frac{v^2}{2{\sigma_v}^2}\right) \mathrm{d}v \tag{2.29}$$

The calculation can be performed as in Section 2.5 with the only addition of the the power-broadened *width parameter* Γ_ν'. This leads to

$$\begin{aligned} \kappa_0' &= h\nu n_0 \frac{\alpha_0}{(1+\frac{2I}{I_s})} \frac{1}{\sqrt{2\pi}\sigma_\nu} \frac{\pi\Gamma_\nu'}{2} = h\nu n_0 \frac{\alpha_0}{(1+\frac{2I}{I_s})} \frac{1}{\sqrt{2\pi}\sigma_\nu} \frac{\pi\Gamma_\nu}{2} \sqrt{1+\frac{2I}{I_s}} \\ &= h\nu n_0 \frac{\alpha_0}{\sqrt{1+\frac{2I}{I_s}}} \frac{1}{\sqrt{2\pi}\sigma_\nu} \frac{\pi\Gamma_\nu}{2} = \frac{\kappa_0}{\sqrt{1+\frac{2I}{I_s}}} \end{aligned} \tag{2.30}$$

and subsequently

$$\kappa = \kappa_0' \exp\left(-\frac{(\nu-\nu_0)^2}{2{\sigma_\nu}^2}\right) \tag{2.31}$$

2.8 Non-linear differential equation

2.9 Data table

		Rubidium	
Isotope	[1]	85	87
Atomic mass	[u]	84.911794	86.909187
10^{-25}	[kg]	1.40999	1.44316
Abundance	[%]	72.17	27.83
Spin I	[1]	$5/2$	$3/2$
Lifetime $6^2P_{3/2}$	[ns]		112
Lifetime $6^2P_{1/2}$	[ns]		125
Wavelength D1-Line ($6^2P_{1/2} \rightarrow 5^2S_{1/2}$)	[nm]	421.5524	
Wavelength D2-Line ($6^2P_{3/2} \rightarrow 5^2S_{1/2}$)	[nm]	420.1792	
$A_{ki,D1},\ \Gamma_{\omega,D1}$	[s^{-1}]	1.50×10^6	
$A_{ki,D2},\ \Gamma_{\omega,D2}$	[s^{-1}]	1.77×10^6	
Natural linewidth $\Gamma_{\nu,D1}$	[MHz]	0.239	
Natural linewidth $\Gamma_{\nu,D2}$	[MHz]	0.282	

Table 2.1 Properties of rubidium isotopes

2.10 D2 line

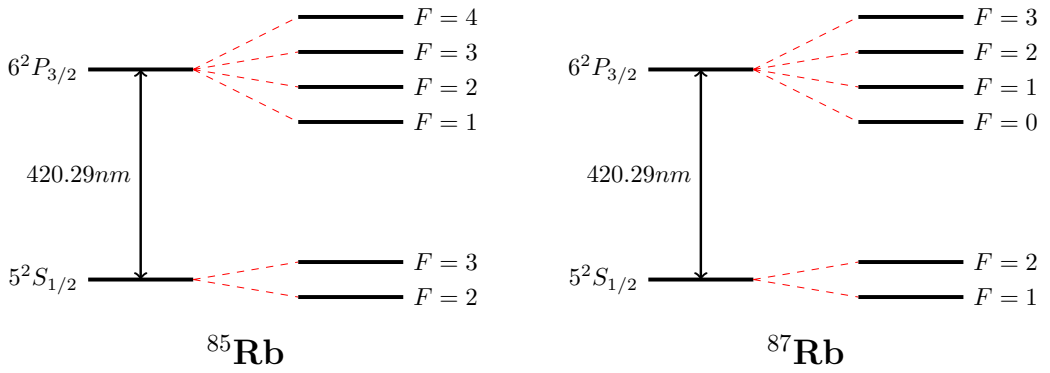

Fig. 2.5 $5^2S_{1/2} \rightarrow 6^2P_{3/2}$ transition of ^{85}Rb and ^{87}Rb with corresponding hyperfine structure

The transition of interest is, as we have discussed before, the $5^2S_{1/2} \rightarrow 6^2P_{3/2}$ of rubidium. As known rubidium occurs in two isotopes, ^{85}Rb and ^{87}Rb. As we can see both isotopes have the same transition energy, but due to the different spin I (see table: 2.1) we get different energy levels for the groundstate [4]. This is the reason why we witness four Doppler peaks in our spectrum.

Caution: Both figures below show the correct correlation between energy and isotopes. The reason for this is that the spectrum shows transition energy and the other one the specific energy levels.

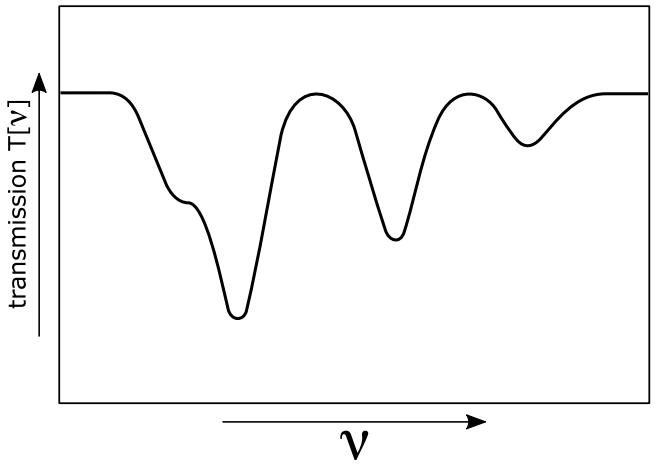

Fig. 2.6 Doppler spectrum of D2 line

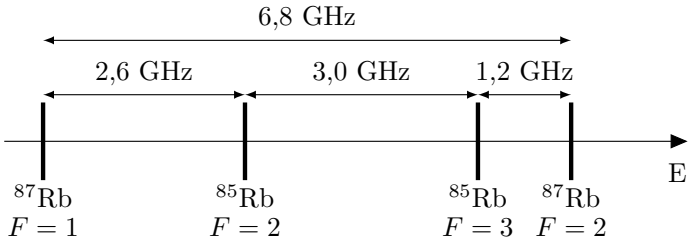

Fig. 2.7 Relative energy gaps of the groundstates between both isotopes

Chapter 3

Experiment

3.1 Setup & Tools

3.2 Laser diameter measurement

3.3 Power / intensity measurement

3.4 Doppler-free measurement

Chapter 4

Evaluation

4.1 Data processing

4.2 Temperature & saturation intensity

4.3 Comparison with theory

4.4 Compare Doppler-free measurement with theoretical values

References

[1] R. Grimm, M. Weidemüller, and Y. B. Ovchinnikov. Optical Dipole Traps for Neutral Atoms. *Advances in Atomic Molecular and Optical Physics*, 42:95–170, 2000.

[2] Department of Physics. Saturated absorption spectroscopy. *University of Florida*, 2001.

[3] Department of Physics. Appendix - saturated absorption spectroscopy. *University of Florida*, 2001.

[4] J. Reader A. Kramida, Yu. Ralchenko and NIST ASD Team (2015). NIST atomic spectra database (ver. 5.3). *National Institute of Standards and Technology*, 2015.

Appendix A

Theory

Appendix B

Experiment

Appendix C

Evaluation